



Dedicated to Academician Cristian Silvestru
on the occasion of his 70th anniversary

THE *IN-SILICO* OPTIMIZATION OF A FED-BATCH REACTOR FOR ETHANOL PRODUCTION BY USING SEVERAL ALGORITHMS

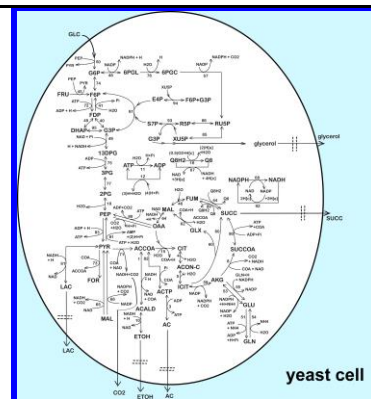
Gheorghe MARIA,^{a,b*} Laura RENEĂ,^a Daniela GHEORGHE^a and Crina MUSCALU^a

^a National University of Science and Technology POLITEHNICA of Bucharest, Dept. of Chemical & Biochemical Engineering, P.O. 35–107, Bucharest, Roumania

^b Roumanian Academy, Chemical Sciences section, Calea Victoriei 125, Bucharest 010071, Roumania.

Received December 4, 2025

Biological production of ethanol is a process well-known from millennia. This biochemical fermentation uses the yeast (*Saccharomyces cerevisiae*) to convert various saccharides (glucose, fructose, sucrose), obtained from various raw-materials, to ethanol on a large production scale. The bioprocess efficiency depends on the yeast exposure through a long period to inhibitors (byproducts), and fluctuations in the quality of the raw materials, etc. Despite tremendous progresses in controlling this bioprocess, the engineering part remains a challenging issue. In this context, engineering tools can help in improving the bioreactor efficiency by implementing suitable optimal operating strategies for a fed-batch bioreactor (**FBR**) case, as studied here. As proved, *in-silico* (math model based) better results are obtained by using an adequate Monod-type process kinetic model adopted from literature, and validated *vs.* extensive experiments. Several **FBR** optimal operating policies, including a constant, or a variable feeding determined with using large/tight searching intervals for the control variables are compared with the aim of maximizing ethanol production, minimizing raw material consumption, and reducing byproduct formation. Various numerical optimization algorithms have been used, by including the Pareto optimal-front technique.



INTRODUCTION

“Biosyntheses spare today a lot of attention to any mean or device improving bioprocess yields. Eventually, they are able to replace the complex chemical processes, which are energetically intensive and generate lot of toxic wastes.^{1,2} In a production chain of producing fine-chemicals, different key-operations are managed and optimized (*i.e.*, cultivation, purification, filtration, biomass immobilization, bioreactor operation, etc.). The fermentative processes conducted in

bioreactors with living cell cultures, or in the enzymatic reactors,¹ are currently used to produce a large variety of valuable molecules,^{3–5} by integrating genetic and engineering methods.^{6,7} Bioreactors are constructed and operated in multiple alternatives as reviewed in the literature.^{5,8}

In spite of their larger volumes, continuously mixed aerated or anaerobic tank reactors, operated in **BR** (batch), or **FBR** (fed-batch) modes, are the most used because they ensure a high oxygen transfer, and a rigorous temperature/pH control, as also the case here for the ethanol (**P**) production.^{5,9–12}

* Corresponding author: gmaria99m@hotmail.com

This work focuses on the engineering part, seeking for production maximization of a **FBR** used for the ethanol biosynthesis, with minimizing the raw-materials consumption, and reducing the excessive formation of byproducts, by using *in-silico* engineering techniques.^{5,13-16}

The *in-silico* derivation of optimal operating policies of a given **FBR** is based on an available bioprocess kinetic model derived from on-/off-line measurements. This model-based optimal operation can be applied in two ways: (a) *off-line* (or 'run-to-run'), by using an adequate extended kinetic model previously identified from the collected experimental data (this paper, and^{5,11,17-19}); (b) *on-line*, by using a simplified, often empirical math model to obtain a state-parameter estimator based on the on-line recorded data (such as the classical Kalman filter).^{16,19-24}

"The use of a deterministic dynamic model, based on the process mechanism, and on macroscopic (measurable) state-variables (as the case here) is preferred due to the physical significance of the terms/parameters, which make possible their validation vs. experimental and literature data, even if repeated model updating is necessary due to the bioprocess variability."²⁹ Typical optimization objective functions were reviewed by Engasser.²⁵

In spite of its low productivity, **BRs** are commonly used for slow bioprocesses, because they are highly flexible and easy to operate in various alternatives.^{5,11,12} In the simple **BR** case, substrate(s), biocatalyst, and additives are initially loaded in the recommended amounts.^{4,12,16,18,26,27,30,31}

"In the **FBR** case, the feeding policy (flow rate, biocatalyst/substrates) are varied following an optimal policy.^{5,9,11,19,20,32} Although, **FBRs** reported better performances compared to other batch alternatives, they are more difficult to operate. That is because they need previously prepared stocks of cell-cultures, and substrate(s), of different concentrations (a-priori *in-silico* determined), to be fed for every 'time-arc' of the batch (that is a batch-time division in which the feeding composition is constant; self-understood, the feeding of time-'arcs' usually differ between them). This is the price paid for achieving **FBR** best performances." Other constructive solutions can be adopted (review of Maria⁵).

The case study approached in this paper refers to the ethanol production from sugars fermentation on yeast. The sugars are obtained from the starch of various crops, mollasses, cellulose, and food

processing byproducts.^{36,37} The literature is plenty with technological details about this old bioprocess,^{37,38} and alternative technologies.^{36,37,39,40}

By using an adequate unstructured (Monod-type) kinetic model from the literature,⁴¹ the *in-silico* analysis of this paper is aiming at evaluating and comparing performances of various alternatives to optimally operate an analyzed **FBR** to maximize the ethanol production from glucose, by using a yeast culture immobilized on millimeter alginate beads.^{42-44,68} The results are also compared with the experimental not-optimal **BR** operation of Zentou *et al.*,⁴¹ and with the not-optimal **FBR** operation of Rivera *et al.*⁴⁵ The paper includes a significant number of elements of novelty, better underlined in the Conclusions section.

EXPERIMENTS TO DETERMINE THE BIOPROCESS KINETIC MODEL

1. The experimental bioreactor and data acquisition

At a cell level, the ethanol is strongly linked to the glycolysis, as long it is produced from the pyruvate, as shown by the simplified core of the central carbon metabolism (**CCM**) in bacteria (Fig. 1), which is similar to those of the yeast given by Teusink *et al.*⁴⁶ As can be seen, beside ethanol, several side-compounds are simultaneously produced (glycerol, AC, SUCC, LAC, and others). To derive a global simplified (Monod type) kinetic model of the sugars fermentation, Zentou *et al.*⁴¹ conducted 6 batch experiments in a **BR** with the characteristics of (Table 1). These experiments run at 30°C, pH 4.5, and for 25 h, covered a large interval of GLC initial concentrations of [25-250] (g/L). The most relevant are those with initial [GLC] of 100, 150, 200 g/L. For each experiment, ca. 8-9 quasi-equidistant samples were taken during the batch to determine the dynamics of the main species: substrate (GLC - S), main product (ethanol - P), the biomass (X), the lump of undesired byproducts (Z). Every kinetic data set was used by Zentou *et al.*⁴¹ to estimate the kinetic model rate constants. Finally, these rate constants are averaged to be valid for the whole interval of the substrate initial concentration. The resulted kinetic model fits very well with the experimental data (figures not presented here, see Zentou *et al.*⁴¹ for details).

In this paper, immobilized biomass on porous millimetric alginate beads have been used, due to their multiple advantages,^{42–44,68} that is: 1) a much higher stability of the biomass; 2) The biomass

(X) can be used as a control variable due to the possibility of being added/removed to/from the **FBR** (an option seldom described in the literature).

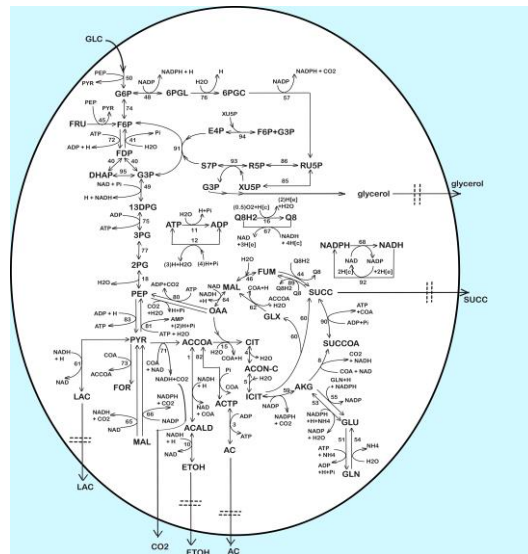


Fig. 1 – Simplified representation of the **CCM** pathway in bacteria of Edwards and Palsson⁶² (including the PTS-system, that is GLCext-to-G6P pathway). Excreted ethanol and its by-products are underlined by separate fluxes. Details on the 95 numbered reactions, involving 72 metabolites, and about the reactions’ stoichiometry, and net fluxes are given by Maria *et al.*⁶³ Adapted from Maria *et al.*⁶³ with the courtesy of CABEQ JI. **GLC** = glucose. See the abbreviation list for species names.

Table 1

The tested operating conditions of the analysed **FBR**. A similar bioreactor was used by Zentou *et al.*⁴¹ in a **BR** mode, and by Rivera *et al.*⁴⁵ in a **FBR** mode to collect kinetic data for the ethanol (P) synthesis by using a culture of yeast.

The BR / FBR conditions		
Control variables	Nominal values	Obs.
Biomass initial concentration, [X] ₀ , (g/L)	10 40–45	Zentou <i>et al.</i> ⁴¹ Rivera <i>et al.</i> ⁴⁵
Feeding immobilized biomass conc. X_j^{feed} (g/L) over the FBR , j = 1, ..., Ndiv	1–100 (tight limits) 1–150 (large limits) Biomass immobilized on alginate beads (this paper)	Optimized within imposed limits (FBR case, eq. 7) Millimetric (1–3) size particles ⁴²
Batch time (Tf), (h.) (aerobic conditions)	25	Zentou <i>et al.</i> ⁴¹
	3	Rivera <i>et al.</i> ⁴⁵
	25	Adopted in this paper
Feed flow-rate (FL) for the FBR case, (L/h)	0.375 (constant, not-optimal)	Rivera <i>et al.</i> ⁴⁵
	0.1–0.5	optimally varied, but not exceeding the reactor capacity
Substrate solution initial conc. [S] ₀ for BR , and feeding solution conc. S_j^{feed} for FBR case, (g/L)	25–250 (BR)	Zentou <i>et al.</i> ⁴¹
	4–18; 172 (FBR)	Rivera <i>et al.</i> ⁴⁵
	25–250 (tight limits) 25–300 (large limits)	To be optimized within imposed limits (eq. 7)
Bioreactor liquid initial / maximum volume (VL), (L)	1	Maximum 2 L ⁴¹
		Maximum 1.5 L ⁴⁵
		Max. 15 L (adopted capacity)
Substrate composition	Glucose (GLC)	This paper; Zentou <i>et al.</i> ⁴¹
	Sugarcane juice (GLC, fructose, sucrose)	Rivera <i>et al.</i> ⁴⁵
Temperature / pH	30°C / 4.5	Zentou <i>et al.</i> ⁴¹ this paper
	28–40°C / 4.5–5	Rivera <i>et al.</i> ⁴⁵
Bioreactor facilities	automatic control pH, DO, temperature	Zentou <i>et al.</i> ⁴¹ Rivera <i>et al.</i> ^{45,48}

Table 2

The dynamic model of the ethanol biosynthesis in the **FBR**. The model combines the mass balance of the bioprocess key-species, and of the **FBR** control variables (GLC, X, FL) for its time step-wise variable feeding policy. The bioprocess kinetic model is those of Zentou *et al.*,⁴¹ with the rate constants estimated from extended experiments carried out in the **BR** of Table 1, and [GLC] initial € [25–250](g/L). Notations: S = GLC = substrate; X = immobilized biomass; P = the desired product (ethanol); Z = the by-products lump, including glycerol, acetate (AC), succinate (SUCC), and lactate (LAC)

Species mass balance (b)	Remarks, and estimated rate constants
<p>Glucose:</p> $\frac{dS}{dt} = \frac{F_{L,j}}{V_L} (S_j^{feed} - S) + r_S;$ <p>S_j^{feed} = control variables to be optimized; j = 1, ..., Ndiv (equal time-arcs); For the optimal FBR with adopted Ndiv =5, the feeding policy is given by eqn.(3). See also the footnote (a).</p> $r_S = -\frac{r_X}{Y_{XS}}$ <p>Biomass:</p> $\frac{dX}{dt} = \frac{F_{L,j}}{V_L} (X_j^{feed} - X) + r_X$ <p>X_j^{feed} = control variables to be optimized; j = 0, ..., Ndiv (equal time-arcs); $r_X = \mu X$;</p> $\mu = \mu_{max,o} \frac{S}{K_S + S} \left(1 - \left(\frac{Z}{Z_m} \right)^{K_Z} \right)$ <p>The main product (ethanol):</p> $\frac{dP}{dt} = \frac{F_{L,j}}{V_L} (P_j^{feed} - P) + r_P$ <p>$r_P = -Y_{PS} r_S$; $P_j^{feed} = 0$ for all j; [P]_o = 0.</p> <p>The lumped by-products (glycerol, AC, SUCC, LAC):</p> $\frac{dZ}{dt} = \frac{F_{L,j}}{V_L} (Z_j^{feed} - Z) + r_Z$ <p>$r_Z = -Y_{ZS} r_S$; $Z_j^{feed} = 0$ for all j; [Z]_o = 0.</p> <p>Liquid volume dynamics:</p> $\frac{dV_L}{dt} = F_{L,j}$ <p>$F_{L,j}$ = control variables to be optimized; j = 0, ..., Ndiv (equal time-arcs);</p>	<p>The bioreactor ideal model main hypotheses are the followings:⁶⁶</p> <ol style="list-style-type: none"> 1).- Isothermal, iso-pH, iso-DO operation (for the aerobic case); 2).- Nutrients, additives, antibiotics, and pH-control compounds⁶⁷ are added initially and during FBR operation to ensure the optimal grow of the biomass; 3).- Aeration in excess (for the aerobic case) over the batch to ensure an optimal biomass maintenance, and to contribute to the liquid homogeneity; 4).- Perfectly mixed liquid phase (with no concentration gradients), of a volume increasing according to the liquid feed flow-rate constant or time-varying policy; 5).- There is a negligible mass resistance for the transport of nutrients / substrates / products / oxygen into the liquid and inside the porous alginate beads; 6).- In the FBR case, the control species (GLC, X) are loaded initially, and then continuously added during the batch according to an optimal variable feeding policy to be <i>in-silico</i> (off-line) determined; 7).- Solid particles of alginate are considered of equal size, and uniformly distributed in the homogeneous liquid phase (perfect mixing conditions). <p>$\mu_{max,o} = 0.244$ (1/h)</p> <p>$K_S = 11.37$ (g/L)</p> <p>$Z_m = 60$ (g/L)</p> <p>$K_Z = 0.83$</p> <p>$Y_{XS} = 0.280$</p> <p>$Y_{PS} = 0.42$</p> <p>$Y_{ZS} = 0.0442$</p> <p>For the adopted Ndiv =5, the feeding policy is given by the eqn.(3). See also the Footnote (a).</p>
<p>Footnote: (a) For the adopted Ndiv = 5, the time-arcs switching points are: T1= 5 h.; T2= 10 h.; T3= 15 h.; T4= 20 h.; $t_f = 25$ h. The $F_{L,0} - F_{L,4}$ time step-wise feed flow-rates are to be determined simultaneously with the other control variables (that is S_j^{feed}, X_j^{feed}) to ensure the FBR optimal operation.</p> <p>(b) The initial concentrations of the key-cell species (S, X), are given in (Table 1).</p>	

2. The proposed kinetic model of Zentou *et al.*⁴¹

This industrial bioprocess is developed at a large scale (over 29.5 billion gallons in 2023 from crops, for food and biofuel industry). Together, the United States and Brazil produce 80% of the world's ethanol.⁴⁷ Due to such a huge importance of this bioprocess, highly intensive efforts were invested in developing an adequate kinetic model aiming at process design, optimization and control.

Among the unstructured (global) models are worth mentioning: Monod;^{41,48,49} Tiessier;⁴⁹ Aiba;⁴⁹ Ghose and Tyagi,⁴⁹ Hinshelwood.⁵⁰ According to Kasbawati⁴⁹ there are no big differences between these models regarding their prediction. Other models try to characterize the dynamics of the simultaneous saccharification-fermentation process for ethanol production.⁵¹ When using a culture of *Zymomonas mobilis*, an oscillatory process is reported, modeled by Escobar.⁵²

Hesitant attempts to extend the validity of the unstructured kinetic models by also including some structural elements referring to the cell metabolism are made by Mazzoleni *et al.*,⁵³ and by Teusink *et al.*⁴⁶

The Monod model adopted in this paper is those proposed by Zentou,⁴¹ being presented in (Table 2) integrated in the **FBR** dynamic model. It was chosen for several reasons: i) it is enough simple to allow quick engineering evaluations, by including only the main four key-species/lumps [S, X, P, Z]; ii) it was proved to be very adequate being fitted and validated over a large number of

data (batch runs). Thus, it was proved to be valid for a large range of initial GLC concentrations.

3. FBR bioreactor model and operating alternatives

To not complicate the numerical evaluations, a simple ideal model of **FBR** was adopted to describe the key-species, and the liquid volume dynamics during the batch at a macroscopic level (**S**, **X**, **P**, **Z**, **V_L** in the bulk, Table 2).

The **FBR** (Fig. 1) ideal model main hypotheses are given in Table 2. The limits of the liquid feed flow-rate ($F_{L,j}$ in eqns. (2,3,4,7)) are adjusted to

not to exceed the bioreactor capacity $\text{Max}(V_L)$ in Table 1. For a variable time step-wise operation, the GLC-substrate S_j^{feed} , and the immobilized

biomass X_j^{feed} are added initially in the bioreactor and during the batch according to an optimal feeding policy to be determined. During the batch $F_{L,j}$ is varied according to an optimal

feeding policy to be determined for every 'time-arc' index 'j' in eqns. (1,3) (that is an interval in which the batch time is divided).

"From a mathematical point of view, in a general form, the **FBR** dynamic model (Table 2) translates to a set of **5** differential mass balances (**ODE** set) written for the key-species of the **FBR**, as followings":⁵

Species in the bulk phase:

$$\frac{dc_i}{dt} = \frac{F_{L,j}}{V_L} (c_{i,j}^{feed} - c_i) \pm r_i(c(t), c_0, \mathbf{k}); c_{i,0} = c_i(t=0)$$

$$c_{P,j}^{feed} = 0, \text{ and } c_{Z,j}^{feed} = 0, \text{ for all } j = 0, 1, \dots, \text{Ndiv}$$

$$\frac{dV_L}{dt} = F_{L,j}; V_{L,0} = V_L(t=0)$$

(1)

where 'i' denotes the considered key-species [S, X, P, Z]; 'j' denotes the **FBR** feeding time-arcs; $j = 1, \dots, \text{Ndiv}$. During the batch $F_{L,j}$ is varied

according to an optimal feeding policy to be determined for every 'time-arc' index 'j' in eq. (1,3,4) (that is an interval in which the batch time is divided). Similarly, the control species 'i' = [GLC, X] are added initially and during the batch

$c_{i,j}^{feed}$ according to an optimal feeding policy to be determined.

The reaction rate r_i expressions together with the associated rate constants are given in the (Table 2). In the above model, c = vector of species concentrations; c_0 = initial value of c (at time $t=0$) given in (Table 1); \mathbf{k} = vector of the model rate constants. The reactor content dilution in eq. (1), determined by the increasing V_L is due to the continuously added F_L term.

In the eqn. (1), S (GLC), X, and F_L are the control variables here.

The optimal **FBR** operation alternatives derived in this paper are more complex than the simple **BR** operation of Zentou,⁴¹ or than the constant not-optimal feeding over the **FBR** batch of Rivera *et al.*⁴⁵

During the batch, the optimal control variables

$$\begin{aligned} F_{L,0} &= F_{L,1} = F_{L,2} = F_{L,3} = F_{L,4} ; \\ c_{GLC,0}^{feed} &= c_{GLC,1}^{feed} = c_{GLC,2}^{feed} = c_{GLC,3}^{feed} = c_{GLC,4}^{feed} ; \\ c_{X,0}^{feed} &= c_{X,1}^{feed} = c_{X,2}^{feed} = c_{X,3}^{feed} = c_{X,4}^{feed} \end{aligned} \quad (2)$$

This case corresponds to the nominal **FBR** not-optimal operating conditions of Rivera *et al.*,⁴⁵ when the control variables $F_{L,j}$ and $c_{GLC,j}^{feed}$ are kept constant.

Of course, a better idea for this alternative (also checked in the present study) is to optimize the initial values of the control variables [$F_{L,0}$; $c_{glc,0}^{feed}$; $c_{X,0}^{feed}$], that is three unknowns by applying a **NLP** procedure (with a single objective function, section 4.2), or a Pareto-optimal front technique (with multiple objectives, section 4.3), both procedures in the presence of imposed search limits, and of multiple constraints (section 4.4). Details on the

$F_{L,j}$, $c_{i,j}^{feed}$ ($i = S, X$) of a **FBR** can be kept constant, or can be variable, according to the following alternatives:

Alternative (A) – constant feeding. A constant feeding along the entire batch, that is (for $N_{div} = 5$):

used **NLP** optimization algorithm and on the Pareto-front are given in the section 4.5.

Alternative (B) – variable feeding. “To not complicate the engineering calculations, the main assumption for a variable feeding of the **FBR** is the following: i) The time-intervals of equal lengths $\Delta t = t_f / N_{div}$ are obtained by dividing the batch time t_f into N_{div} parts $t_{j-1} \leq t \leq t_j$, where $t_j = j\Delta t$ are switching points (where the reactor input is continuous and differentiable), and ii) On each time step-wise arc, index $j=1, \dots, N_{div}$, the control variables are kept constant. Of course, the values on each time-arc do not have to be necessarily equal to each other. Their optimal values are determined from solving an optimization problem (i.e. maximization of the ethanol production here). In math terms, this **FBR** variable operation corresponds to:”⁵⁵

$$c_{i,j}^{feed} = \begin{cases} c_{i,0}^{feed} & \text{if } 0 \leq t < T1 \\ c_{i,1}^{feed} & \text{if } T1 \leq t < T2 \\ c_{i,2}^{feed} & \text{if } T2 \leq t < T3 \\ c_{i,3}^{feed} & \text{if } T3 \leq t < T4 \\ c_{i,4}^{feed} & \text{if } T4 \leq t < t_f \end{cases} ; F_{L,j} = \begin{cases} F_{L,0} & \text{if } 0 \leq t < T1 \\ F_{L,1} & \text{if } T1 \leq t < T2 \\ F_{L,2} & \text{if } T2 \leq t < T3 \\ F_{L,3} & \text{if } T3 \leq t < T4 \\ F_{L,4} & \text{if } T4 \leq t < t_f \end{cases} \quad (3)$$

i index = { GLC, X }

For the adopted $N_{div} = 5$ here, the $j=1, \dots, N_{div}$ time-arcs switching points given in the eq. (3) are the followings: $T1 = t_f / N_{div}$ (5 h.); $T2 = 2 t_f / N_{div}$ (10 h.); $T3 = 3 t_f / N_{div}$ (15 h.); $T4 = 4 t_f / N_{div}$ (20 h.); $t_f = 25$ h.

This variable feeding operation implies a time step-wise variable uneven feeding along the batch (studied in this paper), by *in-silico* (off-line) determining the following control variables (for $N_{div} = 5$ here): $F_{L,0} - F_{L,4}$,

$c_{GLC,0}^{feed} - c_{GLC,4}^{feed}$, and $c_{X,0}^{feed} - c_{X,4}^{feed}$ over the $j = 0, 1, \dots, (N_{div} - 1)$ time-‘arcs’ of the batch, that is $3 \times$

$N_{div} = 15$ unknowns. The optimal operating policy results by applying a **NLP** procedure (with a single objective function, section 4.2) in the presence of imposed search limits, and of multiple constraints (section 4.4). Details on the used **NLP** optimization algorithm are given in section 4.5. Multi-objective **FBR** optimization is possible (not checked in this paper). See Maria and Crisan⁹ as an example.

The major drawback of the **FBR** of variable feeding is coming from its more difficult operation compared to the constant feeding one, as long as the time step-wise optimal feeding policy requires different feeding substrate solution stocks of

different concentrations, and separate different stocks of immobilized biomass of different concentrations, to be fed over the batch. This is the price paid for achieving improved **FBR** performances in most of cases.

The choice of the number of time-‘arcs’ (N_{div}). The **FBR** operating policy with a variable feeding (alternative B) implies a time step-wise variable feeding over an adopted ($N_{div} = 5$ here) equal time-arcs that covers the whole batch time. Each time-arc ‘j’ ($j = 1, \dots, N_{div}$) is characterized by optimal levels of the control variables [$F_{L,j}$; $c_{glc,j}^{feed}$; $c_{X,j}^{feed}$]. This option raises another problem: Which should be the optimal N_{div} in order not to require a large number of feeding stocks of [$F_{L,j}$; $c_{glc,j}^{feed}$; $c_{X,j}^{feed}$] to be prepared in advance, but also to lead to a maximum efficiency of the **FBR**. Besides, **FBR** operation with using a large N_{div} time-arcs can raise special operating problems when including PAT (Process Analytical Technology) tools.⁵⁴

Control variables in a constant feeding operation of the **FBR** (alternative A):

$$[F_{L,0}; c_{glc,0}^{feed}; c_{X,0}^{feed}];$$

Control variables in a time step-wise variable feeding operation of the **FBR** (alternative B):

$$[F_{L,j}; c_{glc,j}^{feed}; c_{X,j}^{feed}] (j = 0, \dots, N_{div})$$

Other parameters of the **FBR** operation are given in (Table 1). Of course, other control variables can be considered as well, that is: temperature,⁴⁸ byproducts intermediate separation,⁴¹ and recovery,⁵⁶ etc.

4.2. Single objective function (Ω) optimization (NLP)

By considering the mentioned control variables eq. (4), optimization of the **FBR** with a constant feeding (alternative A, in Eq.4) consists of *in-silico*

$$\text{Max } \Omega, \text{ where: } \Omega = \text{Max } [\mathbf{P}(t)], \text{ with } (t) \in [0, t_f] \quad (5)$$

The $[\mathbf{P}](t)$ dynamics in eq. (5) is evaluated by solving the **FBR** ODE dynamic model (Table 2) [eq. (1–3)] over the whole batch time ($t) \in [0, t_f]$.

The **NLP** problem eq. (6) is a difficult multi-modal non-convex one, due to the highly nonlinear bioprocess model, and constraints. The problem is solved by applying an effective **NLP** procedure (section 4.5) in the presence of imposed search limits, and of multiple constraints (section 4.4).

A brief survey of the **FBR** optimization literature^{23,55} reveals that a small number ($N_{div}) < 10$ is commonly used due to multiple advantages, extensively pointed-out by Maria.^{5,11} Thus, to not complicate the computational analysis, ($N_{div}) = 5$ was adopted, with equal time-arcs covering the batch time $t_f = 25$ h. Other options are reviewed by Maria.⁵

4. FBR optimization problem

4.1. Control variables selection for the **FBR** optimization

By analysing the **FBR** model of (Table 2), the natural option is to choose as control variables, the ones that are easy to handle, and those that exert a major influence on the bioprocess, according to the kinetic model form. The following control variables are considered for the both operating alternatives (A-B) of the **FBR** (section 3):

(off-line) determining its optimal initial load, simultaneously with its constant optimal feeding policy during the batch leading to maximization of the ethanol $[\mathbf{P}]$ production, eq.(5).

Similarly, optimization of the **FBR** with variable feeding (alternative B, in Eq.4) consists of *in-silico* (off-line) determining its optimal initial load, simultaneously with its feeding policy for every time-interval (‘arc’) during the batch, leading to maximization of the ethanol $[\mathbf{P}]$ production, that is:

4.3. Multi-objective Pareto optimal front for an optimal but constant **FBR** feeding

“When more than one objective function is simultaneously considered, the optimization problem is more difficult to be solved. For multi-objective optimization, several alternatives can be followed.^{57,58} One elegant option is to obtain the set of Pareto optimal solutions, also called Pareto-

front for the case of at least two adverse objectives.⁵⁵ A Pareto solution is one where any improvement in one objective can only take place at the cost of the other objective. In fact, the Pareto-curve is the geometrical place of the all points (problem solutions) that realizes the best compromise between the 2 considered objective functions. The choice of a solution (a point) from this Pareto-curve is subjective, usually depending on other criteria not included in the Pareto-optimization. However, some authors suggested choosing a ‘break point’ of the Pareto-optimal curve as being the most favourable solutions of the optimization problem.”⁵⁵

$$\begin{aligned} & \text{Max. } \mathbf{P} \text{ production –vs.- Min. substrate [S] consumption;} \\ & \text{Max. } \mathbf{P} \text{ production –vs.- Min. inlet biomass [X] feed;} \\ & \text{Max. } \mathbf{P} \text{ production –vs.- Min. feeding flow rate FL (i.e. minimum reactor dilution).} \end{aligned} \quad (6)$$

The problem eq. (6) is solved by applying an effective procedure (section 4.5) in the presence of imposed search limits, and of multiple constraints (section 4.4). Due to the limited efficiency of the used Pareto-optimizer (section 4.5), the rough (slightly oscillating) obtained Pareto-curves are difficult to be interpreted. To better point-out their monotony, approximate Pareto-curves will be generated by using the cubic spline procedure of Matlab with a suitable smoothing constant (section 4.5).

4.4. Optimization problem constraints

The optimization problems eqns. (5–6) are subjected to the following multiple constraints, as followings:

a) The **FBR** dynamic model eq. (1) including the bioprocess kinetic model (Table 2);

For the present case study of a **FBR** operated with a constant optimal feeding eq.(2), several opposite objectives can be considered at the batch end, such as: maximum ethanol (**P**) production, minimum substrate [GLC] consumption, minimum necessary viable biomass $c_{X,j}^{feed}$ to be fed, minimum feed flow rate FL (to avoid a too high dilution of the bioreactor content), and others. Of course, the Pareto-optimal fronts can be obtained by using any pair of these opposite objective functions. In the approached case study, for a **FBR** with an optimal constant feeding, the following four opposite objectives are considered two-by-two, based on their adverse effect in the process model, that is:

- b) The **FBR** running condition from (Table 1), excepting the control variables of eq. (4) which are determined from solving the optimization problem (sections 4.2–4.3);
- c) To limit the excessive consumption of raw-materials, and to account for the limited reactor volume, feasible searching ranges are imposed to the control/decision variables.

To also study the influence of the adopted range size of the control variables on the optimization problem solution quality, two types of the problem constraints have been tested, that is: i) tight search intervals and strong constraints for [X]final and VLfinal (**TISC**), and ii) large search intervals and weaker constraints for [X]final and VLfinal (**LIWC**). In mathematical terms, this idea translates into the following relationships:

Tight search intervals and strong constraints (TISC) (7)

$$\begin{aligned} 25 \text{ (g/L)} & \leq c_{glc,j}^{feed}, [\text{GLC}]_o \leq 250 \text{ (g/L); } \text{VL}_{\text{final}} \leq 10 \text{ L; } [\text{X}]_{\text{final}} < 100 \text{ (g/L)} \\ 1 \text{ (g/L)} & \leq c_{X,j}^{feed}, [\text{X}]_o \leq 100 \text{ (g/L); } 0.1 \text{ (L/h)} \leq F_{L,j}; F_{L,0} \leq 0.5 \text{ (L/h)} \end{aligned}$$

Large search intervals and weak constraints (LIWC)

$$\begin{aligned} 25 \text{ (g/L)} & \leq c_{glc,j}^{feed}, [\text{GLC}]_o \leq 300 \text{ (g/L); } \text{VL}_{\text{final}} \leq 15 \text{ L; } [\text{X}]_{\text{final}} < 150 \text{ (g/L)} \\ 1 \text{ (g/L)} & \leq c_{X,j}^{feed}, [\text{X}]_o \leq 150 \text{ (g/L); } 0.1 \text{ (L/h)} \leq F_{L,j}; F_{L,0} \leq 0.5 \text{ (L/h)} \end{aligned}$$

d) physical meaning of searching variables:

$$F_{L,j} > 0; c_{glc,j}^{feed} \geq 0; c_{X,j}^{feed} \geq 0, \quad (j=1, \dots, N_{\text{div}}) \quad (8)$$

e) physical meaning of state variables:

$$c_i(t) \geq 0, \forall t; \text{ where 'i' = key-species [S, X, P, Z]} \tag{9}$$

The imposed feasible ranges of the control variables in eq. (7) take into account not only the implementation facilities, but also to the economic reasons (minimum substrate consumption, reactor reduced dilution).

4.5. The used numerical solvers

The used numerical solvers are common routines of the Matlab computational package, that is: i) a high-order stiff integrator (ODE15s) to solve the **FBR** dynamic ODE model of (Table 2); ii) an effective genetic algorithm (GAMULTIOBJ) to generate the rough Pareto-optimal fronts (Fig. 2); iii) the (CSAPS) cubic spline procedure to obtain the smoothed Pareto optimal-line, with a suitable smoothing constant.⁶⁹; iv) the multi-modal optimization routine MMA of Maria⁵⁹ has been used to solve the NLP multi-modal, non-convex optimization problem eq. (5), with the constraints eqns. (7–9).

5. Optimization results and discussion

The results obtained by solving the **NLP** optimization problem, and by deriving the Pareto-

optimal fronts, are presented in the following forms:

-.- The Pareto optimal fronts for several opposite objectives (Fig. 2);

-.- The dynamics of the key-species predicted by the adopted kinetic model, for the experimental **BR** of Zentou *et al.*⁴¹ (Table 1) is displayed in Fig. 3. The all **FBR** operating alternatives (that is **NLP**-optimal, or the Pareto-optimal), with a constant or a variable feeding, are comparatively displayed in (Fig. 4, #1–#4);

-.- A comparison of the all **FBR** operating alternatives derived in this paper, and with those from the literature is given in Table 3, in terms of ethanol (**P**) production and raw-materials consumption, even if the batch time of the Rivera *et al.*⁴⁵ experiments is much shorter.

It is to mention that the **FBR** operation in Table 3 is considered in the all operating alternatives (eqns. (1–4)), that is: i) A time step-wise optimal variable feeding (Fig. 4, #1) with **LIWC**; ii) A constant not-optimal feeding (literature results); iii) A constant but optimal feeding (this paper, **NLP**-optimal, or Pareto-optimal), with **LIWC** or **TISC** (Fig. 4, #1–#4).

In the Table 3, the substrate (GLC), and biomass consumption for the **FBR** case was evaluated with the following relationship:

$$m_i = \sum_{j=1}^{N_{div}} c_{i,j}^{feed} F_{L,j} \Delta t_j; \Delta t_j = t_f / N_{div}; \text{ 'i' index = [GLC, X] species} \tag{10}$$

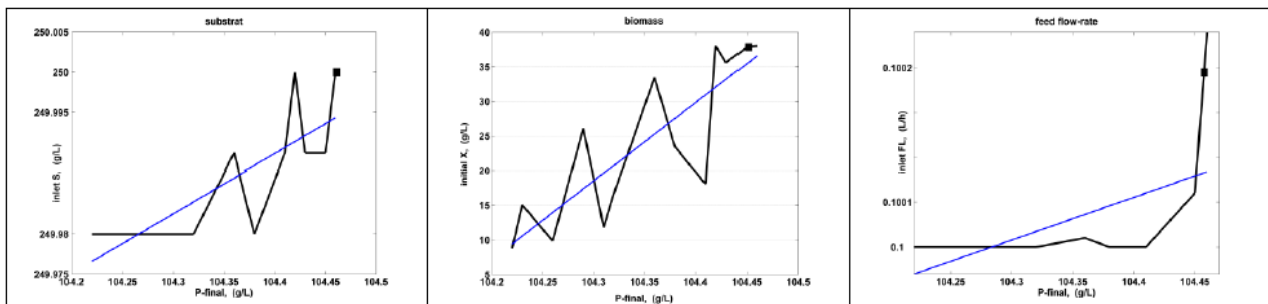


Fig. 2 – The Pareto-optimal fronts for the analyzed **FBR** in terms of pairs of opposite objectives, that is: [LEFT] maximum P production vs. – minimum substrate (GLC) consumption. The end point was chosen as being the most favorable solution (set-point) for this optimization problem. [MIDDLE] minimum fed biomass (X), vs. maximum P production. The marked point corresponds to those of the LEFT Pareto-optimal curve. [RIGHT] required constant feed flow rate (FL), vs. maximum P production. The marked point corresponds to those of the LEFT Pareto-optimal curve. The black curves are the rough Pareto-optimal fronts eq. (6), obtained by imposing tight limits and strong constraints (**TISC**) for the control variables given in eq. (7). The blue lines illustrate the approximated Pareto-optimal fronts by using the cubic spline procedure of Matlab, with a smoothing constant 1e-10.

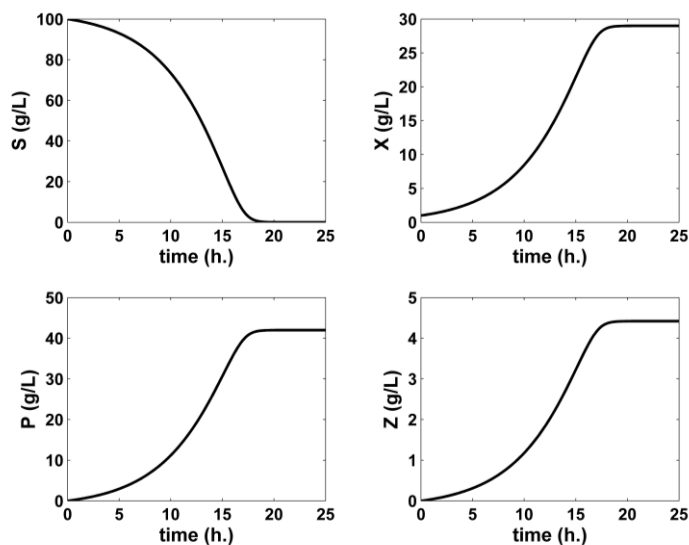


Fig. 3 – Model-based simulated trajectories (—) of the bioprocess key-species (**S**, **X**, **P**, **Z**) in the bioreactor of Zentou *et al.*,⁴¹ operated under nominal, not-optimal batch mode (**BR**) of (Table 1). These predictions fit very well with the plotted experimental data of Zentou *et al.*⁴¹ (not presented here).

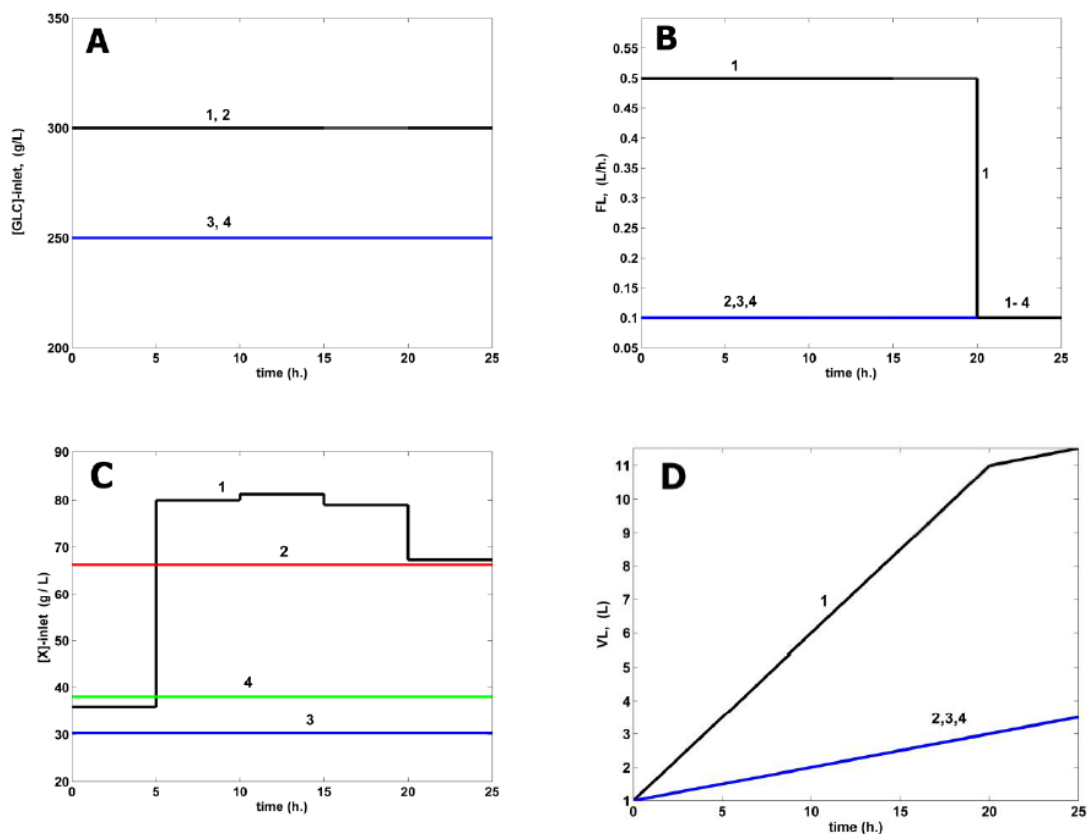


Fig. 4 – Model-based determined [A] optimal feeding with glucose (**GLC**) solution, and [B] optimal feeding flow rate (**FL**), and [C] optimal feeding with immobilized biomass (**X**), and [D] the predicted liquid volume (**VL**) increase in the **FBR** operated under the below #1–4) alternatives.

- #(1) Operation with a time step-wise optimally NLP varied feed flow rate (**FL**), biomass (**X**), and glucose solution (**GLC**), determined with imposing **LIWC** optimization constraints, eq. (7).
- #(2) Operation with a NLP optimal constant feed flow rate (**FL**), and NLP optimal constant concentrations of fed immobilized biomass (**X**), and fed **GLC** solution, with imposing **LIWC** optimization constraints, eq. (7).
- #(3) Operation with a NLP optimal constant feed flow rate (**FL**), and NLP optimal constant concentrations of fed immobilized biomass (**X**), and fed **GLC** solution, with imposing **TISC** optimization constraints, eq. (7).
- #(4) Operation with a Pareto-optimal (Figs. 2–4) constant feed flow rate (**FL**), and Pareto-optimal constant concentrations of fed immobilized biomass (**X**), and Pareto-optimal **GLC** solution, with imposing **TISC** optimization constraints, eq. (7).

By analysing the resulted **FBR** optimal operating policies (plots in Fig. 4), and Table 3) compared to those of the sub-optimal **BR** operation of Zentou *et al.*,⁴¹ or of the sub-optimal **FBR** of Rivera *et al.*,⁴⁵ several observations can be derived, as followings:

1) -.- Irrespectively of its optimal operating policy, the **FBR** efficiency strongly depends on the chosen search intervals for the control (decision) variables, and on the imposed constraints, that is **TISC**, or **LIWC** of eq.(7). Generally, as expected, the **LIWC** optimization conditions lead to **FBR** operating policies of a higher productivity but with the cost of a higher reactor dilution, and a higher biomass production.

2) -.- The kinetic model adopted in this paper fairly fits the experimental data of Zentou *et al.*,⁴¹ being enough adequate to derive engineering evaluations of the **FBR** optimal operation. The simulated key-species dynamics in Fig. 3 (generated by using the Monod model of Zentou *et al.*⁴¹) gives an idea about the low performances of the non-optimized **BR** simple operation.

3) -.- The rough classification given in Table 3 to the different **FBR** operating alternatives (*i.e.* ‘good’, ‘fairly good’, ‘best’) is based on the operating policy performances (ethanol production maximization, raw-materials (GLC,X) minimum consumption, below limit increase of the liquid volume, small production of biomass, small production of byproducts).

4) -.- The best operation alternative is the **FBR** with an optimal variable feeding policy over $N_{div} = 5$ equal time-arcs. Its production is ca. 31x higher than those of the **BR** of Zentou *et al.*,⁴¹ with ca. 31x higher substrate consumption, and with 5x higher production of biomass. Even if the liquid volume increase is significant, another advantage of this policy is given by the lowest percentage of byproducts (0.4%) in the final product, compared to the all other operating alternatives.

5) -.- The efficiency in the ethanol (**P**) production of the NLP optimally operated **FBR** with a variable feeding is significantly higher (1,323 g/25 h) compared to the same **FBR** but with a constant NLP optimal feeding (313.75 g/25 h), with a much lower byproducts content (0.4% vs. 1.7%) for the same biomass production, even if the reactor net dilution is 4.2x higher. The same (**LIWC**) optimization constraints have been used in both cases.

6) -.- The **FBR** with a constant optimal feeding reported a similar efficiency for both Pareto-

optimal, or NLP-optimal operating policy, due to the same **TISC** optimization conditions. By contrast, the same constant feeding but using a NLP-optimal operating policy, with **LIWC** optimization conditions reported better performances, in spite of a higher raw-materials (GLC, X) consumption. This Pareto-optimal set-point was chosen according to the Fig. 2, being the best compromise between maximum P production vs.- minimum substrate (GLC) consumption.

7) -.- Due to the above remarks, it is not surprising that the GLC feeding policy of the **FBR** (Fig. 4A) for the NLP optimally time step-wise varied feeding (FL, GLC, X), is the same with those used for the NLP optimal operation with constant control variables (FL, GLC, X), both cases being obtained with imposing **LIWC** optimization constraints, eq. (7).

8) -.- As remarked by Zentou *et al.*,⁴¹ the byproducts synthesis increases with the inlet GLC concentration. However, the **FBR** with a variable optimal feeding policy (Table 3) reported the smallest percentage content of byproducts (0.4%) due to its variable policy of adding the substrate GLC;

9) -.- Evaluation of the realized yield during the batch for the all compared operating alternatives of Table 3 does not change the established hierarchy mentioned in the column produced P, based on the following criteria: i) maximum productivity in P, simultaneously with ii) minimization of substrate consumption (GLC), and with iii) minimization of formation of secondary products (Z). In all operating alternatives, the realized net yield of ca. 42% is smaller than the theoretical one (ca. 51%). To conclude, the **FBR** with an optimal NLP variable feeding is superior to the other operating alternatives evaluated in Table 3 in many ways, that is: a) the productivity is 4.2–5x higher; b) the percentage of the byproducts (Z) in the product at the batch end is 4x smaller. However, it is fair to also mention the disadvantages of using the **FBR** with an optimal NLP variable feeding. These concern the higher consumption / production of biomass, and a higher reactor content dilution. And, of course, the **FBR** with a variable feeding is more difficult to operate. That is because it needs previously prepared stocks of cell-cultures, and substrate solutions, of different concentrations (*a-priori in-silico* determined), to be fed for every ‘time-arc’ of the batch (that is a batch-time division in which the feeding composition is constant; self-understood, the feeding of time-‘arcs’ usually differ between them).

The **FBR** with a constant not-optimal feeding of Riveira *et al.*⁴⁵ can not be considered in this comparison, because the inlet feed flow rate is not specified by the authors, but only a value used in a previously cultivation step of the yeast. Due to such a reason their yield can not be evaluated.

10) -.- As proved also by the case study of this paper, the optimally operated **FBRs** with a time step-wise variable feeding reported better performances compared to the all other **FBR** operating alternatives. However, they are more difficult to operate. That is because they need previously prepared stocks of immobilized biomass, and substrate(s), of different concentrations (a-priori *in-silico* determined), to be fed for every 'time-arc' of the batch. This is the price paid for achieving **FBR** best performances.^{5,9-12} Besides, **FBR** operation with using a large **Ndiv** time-arcs can raise special operating problems when including PAT (Process Analytical Technology) tools.⁵⁴

CONCLUSIONS

To conclude, the **FBR** operation with an optimal time stepwise control of the feeding policy, or even an optimal constant feeding, but using multiple control variables, reported better performances than the simple **BR** operation due to its higher flexibility in using the biomass and substrates, even if a small number of equal time-arcs is used ($N_{div} < 10$). The major drawback of the **FBR** of variable feeding is coming from its more difficult operation. Besides, **FBR** operation with using a large **Ndiv** time-arcs can raise special operating problems when including PAT (Process Analytical Technology) tools.⁵⁴ An economic global evaluation (not approached here) accounting for the product/raw-material relative value can give a more accurate answer to such a sensitive issue.

The present optimization analysis proves its worth by including multiple elements of novelty. Among others it is to mention: (i) An optimally operated **FBR** with a variable feeding using a small number of time-arcs (< 10), and using wide but feasible ranges for setting the control variables can lead to high performances of the bioreactor. (ii) The major role played by the

variable feeding with the viable biomass, leading to consider (X) as a control variable during **FBR** optimization (an option seldom discussed in the literature). (iii) The **FBR** with an optimal constant feeding could also be an attractive alternative, requiring a much simpler process control, in spite of a much lower productivity due to less need raw-materials. (iv) The **FBR** is considered here with using immobilized biomass, for the reason mentioned in section 2.1. Thus, among others, **FBR** operation with an on-line addition of the viable immobilized biomass (of variable concentration, to be fed for every 'time-arc') is more advantageous, the biomass content becoming a control variable. (v) The advantages of using a reduced, even if unstructured kinetic model, but enough adequate to reproduce the dynamics of the bioprocess key-species to derive quick *in-silico* engineering analyses. Such quick numerical evaluations can be used to base decisions about the best operating policy to be applied to a **BR** or a **FBR** with considering multiple economic goals.

Finally, the **FBR** with an optimal NLP variable feeding, is superior to the other batch / semi-batch operating alternatives, based on the following criteria: i) maximum productivity in P, simultaneously with ii) minimization of substrate consumption (GLC), and with iii) minimization of formation of secondary products (Z). Thus, by reporting the same moderate yield of 42% as in all other alternatives (compared to the theoretical one of 51%), this **FBR** with variable optimal feeding reports better performances in many other ways, that is: a) the productivity is 4.2-5x higher; b) the percentage of the byproducts (Z) in the product at the batch end is 4x smaller. However, it is fair to also mention the disadvantages of using the **FBR** with a variable feeding. These concern the higher consumption / production of biomass, and a higher reactor content dilution. And, of course, it is more difficult to operate. That is because it needs previously prepared stocks of cell-cultures, and substrate solutions, of different concentrations (a-priori *in-silico* determined), to be fed for every 'time-arc' of the batch (that is a batch-time division in which the feeding composition is constant; self-understood, the feeding of time-'arcs' usually differ between them).

Table 3

Efficiency of various operating alternatives of the **FBR**, of (Table 1) in producing ethanol from glucose by using an immobilized yeast culture. Initial liquid volume $V_{L,0} = 1$ L. Notations: **TISC** = Tight search intervals and strong constraints; **LIWC** = Large search intervals and weak constraints, defined by eq. (7). Liquid initial volume $V_{L,o} = 1$ L

Bioreactor operation (B)				Substrate consumption, and biomass production (G)			Produced P			Max [Z]	Final $V_{L,f}$
Type	N_{div}			GLC (%Z)	Biomass (X)		[P]f, (g/L)	Net [P]f × ΔV_L (g)	Net Yield (%) (H)	(g/L)	(Net ΔV_L) (J) (L)
					Consumed (g)	Final (g/L)					
BR Experiments of Zentou et al. ⁴¹	1	Nominal initial load (Fig. 3)		100 (9.5%)	1	29	42	42 (poor)	42	4.42	1 (0)
		[GLC]in	100								
		[X]in	1								
		[P,Z]in	0								
		Tf	25 h								
FBR Constant not-optimal feeding of Riveira et al. ⁴⁵	1	FL = 0.375 L/h (?) [GLC]feed = 15.52		17.46 (?%)	50.4	30	14.6	1.825	?	?	1.125 (0.125)
		[GLC]in	15.52								
		[X]in	44.83								
		[P,Z]in	0								
		Tf	3 h								
FBR NLP optimal variable feeding, (this paper)	5	Fig. 4 (LIWC) ; (D)		3,149 (0.4%)	723	150	126	1,323 (best)	42	13.24	11.5 (10.5)
		[GLC]in,o	300								
		FL,in,o	0.5								
		[X]o	35.84								
		[P,Z]o	0								
		Tf	25 h								
FBR Constant, but NLP optimal feeding, (this paper)	1	Fig. 4 (LIWC) ; (E)		750 (1.7%)	166	150	125.5	313.75 (fairly good)	42	13.2	3.5 (2.5)
		[GLC]initial	300								
		FL, initial	0.1								
		[X]initial	66.31								
		[P,Z]in	0								
		Tf	25 h								
FBR Constant, but NLP optimal feeding, (this paper)	1	Fig. 4 (TISC); (E)		625 (1.7%)	76	100	104.4	261 (good)	42	10.98	3.5 (2.5)
		[GLC]in, initial	250								
		FL, initial	0.1								
		[X]initial	30.38								
		[P,Z]in	0								
		Tf	25 h								
FBR Constant, but Pareto-optimal	1	Fig. 4 (TISC); (F)		626.5 (1.7%)	95.22	107.6	106	265	42.3	11.0	3.5
		[GLC]in,	250								

Greeks μ

Rate constant

 Ω **FBR** optimization objective function, eq. (5)**Subscripts**

0,o

Initial

cell

Referring to the (inside) cell

ext

External to cell (*i.e.* in the bulk phase)

F, final

Final

in

In the feed (inlet)

x

Biomass

Abbreviations

13dpg, pgp

1,3-diphosphoglycerate

3pg

3-phosphoglycerate

2pg

2-phosphoglycerate

AA

Amino-acids

Accoa, acetyl-CoA

Acetyl-coenzyme A

AC

Acetate

ACALD

Acetaldehyde

ACON-C

Aconitate

ACTP

Acetate permease

ADP, adp

Adenosin-diphosphate

AK-ase

Adenylate kinase

AKG

Alfa-ketoglutarate

ALE

Adaptive laboratory evolution

AMP, amp

Adenosin-monophosphate

ATP, atp

Adenosin-triphosphate

ATP-ase

ATP monophosphatase

CCM

Central carbon metabolism

CIT

Citrate

DO

Dissolved oxygen

DW

Dry mass

E

Enzyme anthranilate synthase in the TRP synthesis model.

ETOH

Ethanol

ext

External to the cell (*i.e.* in the bulk phase)

E4P

Erythrose 4-phosphate

FBR

Fed-batch bioreactor

FDP, fdp

Fructose-1,6-biphosphate

F6P, f6p

Fructose-6-phosphate

FUM

Fumarate

GalP/Glk

Galactose permease/glucokinase

G3P, g3p, GAP,

Glyceraldehyde-3-phosphate

gap, 3PG, 3pg

2PG, 2pg

2-phosphoglycerate

G6P, g6p

Glucose-6-phosphate

GLC, glc

Glucose

Glc(ex), [GLC]ext

Glucose in the environment (bulk phase)

GLN

Glutamine

GLU

Glutamate

GMO

Genetic modified micro-organisms

GRC

Genetic regulatory circuits

HK-ase

Hexokinase

ICIT

Isocitrate

JWS

Silicon Cell project of Olivier and Snoep⁶¹

LAC, lac

Lactate

MACR

Mechanically agitated continuously aerated reactor

MAL

Malate

Max (x)

Maxim of (x)

MMA

The adaptive random optimization algorithm of Maria⁵⁹

MRNA

Tryptophan messenger ribonucleic acid during its encoding gene dynamic transcription, and translation

NAD(P)H

Nicotinamide adenine dinucleotide (phosphate) reduced

NLP

Nonlinear programming

OAA	Oxaloacetate
ODE	Ordinary differential equations set
OR	The complex between O and R (aporepressor of the TRP gene)
OT	The total TRP operon
P, Pi	Phosphoric acid
PEP, pep	Phosphoenolpyruvate
13DPG=PGP	1,3-diphosphoglycerate
<i>PFK-ase</i>	Phosphofruktokinase
PK-ase	Pyruvate kinase
PTS	Phosphotransferase, or the phosphoenolpyruvate:glucose phosphotransferase system
PYR, pyr	Pyruvate
QSS	Quasi-steady-state
Q8	Ubiquinone-8
Q8H2	Ubiquinol-8
R5P	Ribose 5-phosphate
RU5P	Ribulose 5-phosphate
mRNA, MRNA	Messenger ribonucleic acid; tryptophan mRNA during its encoding gene dynamic transcription, and translation
SUCC, suc	Succinate
SUCCOA	Succinyl-CoA
S7P	Sedoheptulose 7-phosphate
TCA, tca	Tricarboxylic acid cycle
TF	Gene expression transcription factors
TRP, Trp, trp	Tryptophan
XU5P	Xylulose 5-phosphate
X	Biomass
Wt.	Weight
[.]	Concentration

REFERENCES

1. A. Liese, K. Seelbach and C. Wandrey, "Industrial biotransformations", Wiley-VCH, Weinheim, 2006.
2. J. A. Moulijn, M. Makkee and A. van Diepen, "Chemical process technology", Wiley, New York, 2001.
3. M. A. Henson, in "The control handbook", W. Levine (Ed.), 2nd edition. Taylor and Francis, New York, 2010.
4. L. Dewasme, F. Cote, P. Filee, A.L. Hantson, and A.V. Wouwer, *Bioengineering (Basel)*, **2017**, *4*, 17. doi:10.3390/bioengineering4010017
5. G. Maria, *Molecules – Organic chemistry (MDPI)*, **2020b**, *25*, 5648–5674, doi:10.3390/molecules25235648
6. K. Buchholz, and D.C. Hempel, *Eng. Life Sci.*, **2006**, *6*, 437–437. <https://doi.org/10.1002/elsc.200690012>
7. D.C. Hempel, *Eng. Life Sci.*, **2006**, *6*, 443–447. <https://doi.org/10.1002/elsc.200620149>
8. V. Nedovic, and R. Willaert, „Applications of cell immobilisation technology, Springer verlag, Amsterdam, **2005**.
9. G. Maria, and M. Crisan, *J. Process Control.*, **2017**, *53*, 95–105. doi: 10.1016/j.jprocont.2017.02.004
10. M.G. Avili, M.H. Fazaelpoor, S.A. Jafari, and S.A. Ataei, *Iranian Journal of Biotechnology*, **2012**, *10*, 263–269.
11. G. Maria, and L. Renea, *Bioengineering-Basel-MDPI*, **2021**, *8*, 210–247, <https://doi.org/10.3390/bioengineering8120210>
12. G. Maria, and I.M. Peptanaru, *Dynamics-Basel-MDPI*, **2021**, *1*, 134–154, <https://doi.org/10.3390/dynamics1010008>
13. P. Agrawal, G. Koshy, and M. Ramseier, *Biotechnol. Bioeng.*, **1989**, *33*, 115–125. doi: 10.1002/bit.260330115
14. A. Ashoori, B. Moshiri, A. Khaki-Sedigh, and M.R. Bakhtiari, *Journal of Process Control*, **2009**, *19*, 1162–1173. <https://doi.org/10.1016/j.jprocont.2009.03.006>
15. J.R. Banga, A.A. Alonso, and P.R. Singh, *AIChE Annual Meeting*, San Francisco, Nov. 13–18, **1994**.
16. D. Bonvin, Real-time optimization, MDPI, Basel, **2017**.
17. G. Maria, *Comput. and Chemical Eng.*, **2021a**, *133*, 106628–106635. <https://doi.org/10.1016/j.compchemeng.2019.106628>
18. B. Srinivasan, C.J. Primus, D. Bonvin, and N.L. Ricker, *Control Engineering Practice*, **2001**, *9*, 911–919.
19. R. Mendes, I. Rocha, J.P. Pinto, E.C. Ferreira, and M. Rocha, In: „Advances in differential evolution. Studies in Computational Intelligence, U.K. Chakraborty, (Ed.), Springer verlag, Berlin, **2008**; pp. 299–317.
20. D. DiBiasio, In: Chemical Engineering Problems in Biotechnology, M.L. Shuler, (Ed.); AIChE, New York, **1989**, vol. 1.
21. J. Lee, K.S. Lee, J.H. Lee, and S. Park, *Control Eng. Pract.*, **2001**, *9*, 901–909. [https://doi.org/10.1016/S0967-0661\(01\)00052-1](https://doi.org/10.1016/S0967-0661(01)00052-1)
22. D. Ruppen, D. Bonvin, and D.W.T. Rippin, *Comput. Chem. Eng.*, **1998**, *22*, 185–199. [https://doi.org/10.1016/S0098-1354\(96\)00358-4](https://doi.org/10.1016/S0098-1354(96)00358-4)
23. C. Loeblein, J. Perkins, B. Srinivasan, and D. Bonvin, *Comput. Chem. Eng.*, **1997**, *21*, S867–S872. [https://doi.org/10.1016/S0098-1354\(97\)87611-9](https://doi.org/10.1016/S0098-1354(97)87611-9)
24. M. Rao, and H. Qiu, Process control engineering: A textbook for chemical, mechanical and electrical engineers, Gordon and Breach Science Publ., Amsterdam, **1993**.
25. J.M. Engasser, *Chem. Eng. Sci.*, **1988**, *43*, 1739–1748. [https://doi.org/10.1016/0009-2509\(88\)87038-6](https://doi.org/10.1016/0009-2509(88)87038-6)
26. G. Maria, *Comput. Chem. Eng.*, **2020**, *133*, 106628–106635. <https://doi.org/10.1016/j.compchemeng.2019.106628>

27. C. Wang, H. Quan, and X. Xu, *Ind. Eng. Chem. Res.*, **1996**, *35*, 3560–3566, <https://doi.org/10.1021/ie9506633>
28. S.S. Ozturk, and B.O. Palsson, *J. Biotechnol.*, **1990**, *16*, 259–278. [https://doi.org/10.1016/0168-1656\(90\)90041-9](https://doi.org/10.1016/0168-1656(90)90041-9)
29. J. Fotopoulos, C. Georgakis, and H.G. Stenger jr., *Chem. Eng. Sci.*, **1994**, *49*, 5533–5547
30. E. Martinez, *Proc. 2nd Mercosur Congress on Chemical Engineering*, Rio de Janeiro, Costa Verde, Brasil, **2005**, paper #20.
31. J.C. Binette, and B. Srinivasan, *Processes*, **2016**, *4*, 27. doi: 10.3390/pr4030027
32. I.Y. Smets, J.E. Claes, E.J. November, G.P. Bastin, and J.F. Van Impe, *Jl. Process Control*, **2004**, *14*, 795-805. doi:10.1016/j.jprocont.2003.12.005
33. D. Sarkar, and J.M. Modak, *Chem. Eng. Sci.*, **2005**, *60*, 481–492. <http://dx.doi.org/10.1016/j.ces.2004.07.130>
34. G. Maria, Hybrid modular kinetic models linking cell-scale structured CCM reaction pathways to bioreactor macro-scale state variables. Applications for solving bioengineering problems, Juniper publ., Irvine, California (USA), **2023**.
35. G. Maria, and I. Luta, *Comput. Chem. Eng.*, **2013**, *58*, 98–115. doi: 10.1016/j.compchemeng.2013.06.004.
36. M. Kanagasabai, B. Elango, P. Balakrishnan, and J. Jayabalan, In: R. Pandey, I. Pala-Rosas, J.L. Contreras, and J. Salmones, *Ethanol and Glycerol Chemistry – Production, Modelling, Applications, and Technological Aspects*, IntechOpen, London (UK), **2023**. doi: 10.5772/intechopen.102260
37. M.Y. Akbas, and B.C. Stark, *Jl. Ind. Microbiol Biotechnol*, **2016**, *43*, 1593–1609, DOI 10.1007/s10295-016-1821-z
38. N. Macedo, and C.J. Brigham, *Intl. Jl. Biotechnology for Wellness Industries*, **2014**, *3*, 79–87.
39. G. Maiorella, H.W. Blanch, and C.R. Wilke, *Biotechnology and Bioengineering*, **1983**, *XXV*, 103–121.
40. H. Li, X. Mei, B. Liu, Z. Li, B. Wang, N. Ren, and D. Xing, *Environment International*, **2019**, *129*, 1–9, <https://doi.org/10.1016/j.envint.2019.05.013>
41. H. Zentou, Z.Z. Abidin, R. Yunus, D.R.A. Biak, M.A. Issa, and M.Y. Pudza, *ACS Omega*, **2021**, *6*, 4137–4146, <https://dx.doi.org/10.1021/acsomega.0c04025>
42. M.D.N. Ramos, J.P. Sandri, A. Claes, B.T. Carvalho, J.M. Thevelein, T.C. Zangirolami, and T.C. Milessi, *New Biotechnology*, **2023**, *78*, 153–161.
43. P.M. Doran, and J.E. Bailey, *Biotechnol. Bioeng.*, **1986**, *28*, 73-87. doi: 10.1002/bit.260280111.
44. A.D. Garcia-Villagomez, J. Galindo-de-la-Rosa, A. Dector, A. Alvarez, J.A. Rodriguez-Morales, J.M. Olivares-Ramirez, N. Arjona, A.U. Chavez-Ramirez, and V. Vallejo-Becerra, *Intl. Jl. Hydrogen Energy*, **2023**, *48*, 5301–5312.
45. E.C. Rivera, C.K. Yamakawa, M.H. Garcia, V.C. Geraldo, C.E.V. Rossella, R.M. Filho, and A. Bonomi, *Chemical Engineering Transactions*, **2013**, *32*, 1369–1374. doi: 103303/CET1332229
46. B. Teusink, J. Passarge, C.A. Reijenga, E. Esgalhado, C.C. van der Weijden, M. Schepper, M.C. Walsh, B.M. Bakker, K. van Dam, H.V. Westerhoff, and J.L. Snoep, *Eur. J. Biochem.*, **2000**, *267*, 5313–5329. doi: 10.1046/j.1432-1327.2000.01527.x
47. Statista inc., New York, **2024**, <https://www.statista.com/contact/>
48. E.C. Rivera, A.C. Costa, D.I.P. Atala, F. Maugeri, M.R.W. Maciel, and R.M. Filho, *Process Biochemistry*, **2006**, *41*, 1682–1687, doi:10.1016/j.procbio.2006.02.009
49. S.R. Kasbawati, S.A.K. Jaya, and A. Kalondeng, *Biotechnology & Biotechnological Equipment*, **2018**, *32*, 1167–1173, doi: 10.1080/13102818.2018.1503563
50. H. Jin, R. Liu, and Y. He, *Procedia Environmental Sciences*, **2012**, *12*, 137–145, doi: 10.1016/j.proenv.2012.01.258
51. S. Ochoa, A. Yoo, Y.U. Repke, G. Wozny, and D.R. Yang, *Biotechnol. Prog.*, **2007**, *23*, 1454–1462, doi: 10.1021/bp0702119
52. N.P. Escobar, P.A. Saldarriaga-Aristizábal, and V. Chaparro-Muñoz, *Revista Facultad de Ingenieria, Universidad de Antioquia*, **2018**, *88*, 26–39.
53. S. Mazzoleni, C. Landi, F. Carteni, E. Alteriis, F. Giannino, L. Paciello, and P. Parascandola, *Microb Cell Fact*, **2015**, *14*, 109, doi 10.1186/s12934-015-0295-4
54. A. Bharat, Process analytical technology (PAT), *Msc. Diss.*, P.D.V.V.P.F.S. College of pharmacy, AhmedNagar (India), **2013**.
55. A. Dan, and G. Maria, *Chemical Eng. and Technol.*, **2012**, *35*, 1098–1103. doi: 10.1002/ceat.201100706.
56. T.J. Tse, D.J. Wiens, F. Chicilo, S.K. Purdy, and M.J.T. Reaney, *Fermentation*, **2021**, *7*, 267. <https://doi.org/10.3390/fermentation7040267>
57. D. Nagrath, M. Avila-Elchiver, F. Berthiaume, A.W. Tilles, A. Messac, and M.L. Yarmush, *Metab Eng.*, **2010**, *12*, 429–445. doi: 10.1016/j.ymben.2010.05.003.
58. S.S. Rao, *Engineering optimization – Theory and practice*, Wiley, New York, **2009**. Chapter 14.10.G. Maria, In: *Modelling, Identification and Control*, M.H. Hamza, (Ed.), IASTED/ACTA Press, Anaheim (CA), **2003**, pp. 112–117.
60. J. Becker, and E. Boles, *App. and Env. Microbiology*, **2003**, *69*, 4144–4150, doi: 10.1128/AEM.69.7.4144–4150.2003
61. B.G. Olivier, and J.L. Snoep, *Bioinformatics*, **2004**, *20*, 2143–2144. DOI: 10.1093/bioinformatics/bth200
62. J.S. Edwards, and B.O. Palsson, *Proc. Natl. Acad. Sci. USA*, **2000**, *97*, 5528–5533. doi: 10.1073/pnas.97.10.5528
63. G. Maria, Z. Xu, and J. Sun, *Chemical and Biochemical Engineering Quarterly*, **2011**, *25*, 403-424.
64. M. Bishop, An introduction to chemistry, Chiral publ., **2013**. https://preparatorychemistry.com/Bishop_contact.html
65. K. Laos, and M. Harak, *J. Food Physics*, **2014**, *27*, 27–30.
66. A. Moser, „Bioprocess technology - kinetics and reactors, Springer Verlag, Berlin, 1988.
67. M. Chen, Novel approaches for in vivo evolution, screening and characterization of enzymes for metabolic engineering of *Escherichia coli* as hyper L-tryptophan producer, *PhD thesis*, TU Hamburg, **2020**.
68. J. Moreno-Garcia, T. García-Martínez, J.C. Mauricio, and J. Moreno, J., *Frontiers in Microbiology*, **2018**, *9*, article 241, <https://doi.org/10.3389/fmicb.2018.00241>
69. G. Maria, and D. Gheorghie, *Algorithms – Basel-MDPI*, **2024**, *17*, 428–468. <https://doi.org/10.3390/a17100428>

